Proceedings of the 2nd ICEENG Conference, 23-25 Nov. 1999 | AW-2 | 1

Military Technical College
Kobry Elkobbah,
Cairo, Egypt

ICEENG 99

2nd International Conference on
Electrical Engineering
ICEENG 99

A study of refractive multi path fading on microwave LOS links in Syria

Mohamed A. H. Eleiwa, Odai M. Nadeem, Alaa Fahmy, and A. A. Mitkees
Military Technical College, Cairo, Egypt

Abstract

Refractive multi path fading is recognized as the dominant mechanism of system degradation on MLOS (Microwave Line Of Sight) links. Therefore the objectives of the proposed propagation study in this paper are to obtain quantitative estimates describing the possible propagation mechanisms through a tropospheric region, and to predict the performance of proposed MLOS links in that region. Various measurements on temperature, relative humidity, and pressure are recorded for a humid region (Homs), and supplied by meteorological department in Syria. The data is based on daily measurements ranging from 3 to 8 readings with a collection period of 3 years (1994,95,96). Knowing the meteorological conditions, the profile of refractivity is first determined in that region. The mathematical model of the propagation channel is then generated to calculate the multi path parameters. Different link parameters and configurations are also proposed , and the performance of each is analyzed. Consequently, the optimum link parameters and configuration are recommended.

I- Introduction

Owing to the irregular and changing nature of the propagation medium and interference among waves traveling along different paths, the received signal amplitude fluctuates or fades. Fading can be categorized as multi path, atmospheric absorption, and scattering loss. Refractive multi path fading is the most serious type and it is the result of electromagnetic waves bending over multiple paths.

Theoretical and empirical models [1,2,3] have been used to study the mechanism of multi path fading. The theoretical model presented in [1] was devised to deal only with equal transmitter and receiver antenna heights. The effect of the earth's curvature has been considered by the models presented in [2,3], but to deal only with specific link configurations.

In this paper, the model of [2] has been extended to analyze the performance of all possible link configurations [4]. The analysis in this study is based on a set of data base provided by the meteorological department in Syria. Various measurements on temperature, humidity, and pressure in a humid area (Homs) are recorded. Refractivity and its gradient are first calculated from the measured data. The vertical refractivity

profiles are then plotted, and the numerical model is finally applied to characterize the proposed MLOS links in that region.

II- Refractivity profile calculations

The data is based on daily measurements ranging from 3 to 8 readings with a collection period of 3 years (1994,95,96). The monthly average dry bulb temperature t(^{o}c), relative humidity H_r%, and station pressure P(mb) are presented in tables 1,2, and 3; respectively.

The refractivity N is first calculated by substituting the measured values in the following semi-empirical formulae [5]

$$N = 77.6\frac{P}{T} + 3.73\times10^5\frac{e}{T^2} \quad (1)$$

$$e = \frac{H_r}{100}\left[6.1121\exp\left(\frac{17.502t}{t+240.97}\right)\right] \quad (2)$$

The first term of the right hand side of (1) is termed the dry term (DT), while the second term is called the wet term (WT). In hot and humid areas, large variations in the WT term are observed. The monthly variation of N is shown in Fig.1, where N_{max}=335 is obtained for summer months (July, August, and September), while N_{min}=305 is obtained in winter months. The average refractivity is shown in Fig.2. The modified refractive index M for a flattened earth is given by

$$M(z) = N(z) + (z/a)10^6 \quad (3)$$

where a=6372.75 km is the radius of the earth, and z is the vertical height above the earth's surface.

The anomalies in the meteorological parameters are observed at 4 hours period beginning at t_a=22:30 and t_b=22:55 on May 25th, and t_c=00:15 and t_d=00:35 on May 26th, 1996. When the data measured using tethered balloon, the height z was measured w.r.t. the ground level. The refractivity indices N and M are then calculated using (1) and (3); respectively, and the refractivity vertical profiles for N and M are plotted in Figs. 3 and 4; respectively. These figures show the formation of elevated ducting (inversion) layers (gradient steeper than 157 Nu/km) at height z=84 m with dN/dh=-400 Nu/km and dN/dh=-370 Nu/km at t_a=22:30 and t_b=22:55; respectively. This is probably due to the strong advection of humidity from the lake located at the west of Homs. Having the M-curves (the variation of M with height) in Homs region, it is now possible to characterize the multi path rays for MLOS links in that region using the following numerical model.

III- Refractive multi path numerical model

To preserve the relative curvature between the rays and the flattened earth, the modified ray paths are approximated with circular arcs of radius R, which is given by

$$R\big|_{km} = \frac{10^6}{\left[\frac{-dM}{dz}\right]_{Nu/km}} \quad (4)$$

In the standard troposphere region, where M has a positive slope with height, the rays are

curved upward with $R=R_f$. Upon entering the inversion layer at height h_L, the radius of curvature becomes 1/R downwards.

The multi path parameters (delay time $\tau\tau$, power factor PF, launching angle θ_t, and receiving angle θ_r) are determined using computer programs developed on the basis of the analysis presented in [2]. The delay time τ for each ray is found by integrating the modified refractive index m along the path as

$$\tau = \frac{1}{c}\int m ds \qquad (5)$$

where $ds=Rd\theta$ is the differential arc length. The ratio of the received to transmitted power is given by the power factor PF as

$$PF = \frac{\cos\theta_t}{L\sin\theta_r}\frac{d\theta_t}{dL} \qquad (6)$$

where L is the ground link range.

As an example, consider the link geometry shown in Fig.5 with the highest terminal (receiving one) is above the inversion layer interface. Performing the tegration of (5) over every ray segment in Fig.5, and dividing by the light speed c to obtain the time delay as in the following equation (7)

$$\tau = \frac{R}{c}\left[\theta_r(1+\cos\theta_t)-\sin\theta_r\right]-\frac{R_f}{c}\left[\theta_t(1+\cos\theta_t)-\sin\theta_t\right]+(2n+1)\frac{R+R_f}{c}\left[\theta_t(1+\cos\theta_t)-\sin\theta_t\right]$$

Using the geometry of Fig.5 with (6) to get the following expression for the power factor PF as

$$PF = -\left(\frac{R}{LR_fK_r}\right)\left(\frac{\partial K_t}{\partial L}+\frac{K_t}{L}\right) \qquad (8)$$

where $\frac{\partial K_t}{\partial L} = \frac{4\rho^2K_rC_n(A+S)-2A\left(\frac{K_t}{2}-1\right)}{L\left(8\rho^2C_nK_rK_t-Q_0\right)}$, $K_r = 2R\sin\theta_r/L$, $K_t = -2R_f\sin\theta_t/L$,

$A,S = \frac{8R_f}{L^2}\left[h_L-h_t\mp\rho(h_r-h_L)\right]$, $C_n = \frac{(2n+1)^2(R+R_f)^2}{8R_f^2}$, $\rho = R_f/R$, and

$Q_n = -\frac{A}{2}+2C_n(A-S)$. Finally, the transmit and receive angles can be determined by solving the following two equations simultaneously:-

$$K_r^2\rho^2-K_t^2 = A \qquad (9)$$

$$K_r^2\rho^2-\frac{1}{C_n}\left(\frac{K_r+K_t}{2}-1\right)^2+K_t^2 = -S \qquad (10)$$

V- MLOS link analysis

The developed numerical model in the previous section is then applied to study a line of sight link situated in Homs. The proposed link characteristics are link distance L=50km, transmitting antenna height h_t=80m, receiving antenna height h_r=90m, antenna gain G=36dB, antenna beamwidth HPBW=2.64°, and the operating frequency f=4.6GHz.

The variation of M with height at different times, as shown in Fig.4, shows that the standard refractive conditions prevail during the day time(t_c=00:15, and t_d =00:35). Under these conditions of a well-mixed atmosphere, the received signal is mainly due to the direct ray as shown in Figs. 6 and 7. After sunset, the inversion layers are formed at t_a =22:30 , and t_b =22:55 as a result of the radiation cooling of the earth's surface. The multi path rays are therefore resulting as shown in Figs. 8 and 9. Fig.8 shows two rays, one with launching angle θ_t=-0.1098° and sags to altitude 59m, while the other is launched at θ_t=-0.09167° and sags to altitude 65m. At time t_b =22:55 Fig.9 exhibits only one ray. To study the frequency selectivity of refractive multi path fading, its amplitude |T(f)| is then calculated at fixed time , but function in frequency f as given by

$$T(f) = \sum_{i=1}^{N} \alpha_i \exp(-j2\pi f \tau_i) \qquad (11)$$

where $\alpha = \sqrt{PF}$ is the ray path amplitude, while τ is the ray delay. The fading level |T| is calculated for the two refracted rays shown in Fig.8, and the resulting frequency dependence is shown in Fig.10, where an 8dB variation in the fading level is noticed within a 30MHz band and with deep fading level at f= 4.593GHz.

V-Conclusion

Meteorological measurements for Homs region in Syria shows refractivity change creating inversion layers at some hours during night. Computer programs have been developed to characterize multi path fading over a two-layer tropospheric model with an elevated duct. The developed numerical model has been applied to analyze refractive multi path fading over a proposed MLOS link located near the humid region of Homs in Syria. Multi path rays have been plotted and their parameters have been calculated. Also, the frequency selectivity of fading has been studied, and hence the particular combinations of link parameters yielding deep fading could be avoided.

VI- References

[1] C.L.Ruthroff,"Multiple-path fading on line-of-sight microwave radio systems as a function of path length and frequency," BSTJ, Vol. 50, pp.2375-2398, September 1971.

[2] L. W. Pickering, and J. Derosa, "Refractive multipath model for line-of-sight microwave relay links," IEEE Trans. on Communications,Vol. COM-27, No.8, August 1979.

[3] S. F. Mahmoud, H. N. Boghdadi, and O.L. El-Sayed, "A theoretical model for multipath fading on line of sight propagation," 3rd NRSC, pp.320-334, Cairo-Egypt, Feb. 1985.

[4] Odai M. N. Ali, "Microwave communications systems (microwave link)," M.Sc.thesis, M.T.C., Cairo, 1998.

[5] John Griffiths, "Radio wave propagation and antennas, an introduction," School of ectrical Engineering, University of Bath, U.K., 1987.

Table 1. Monthly average daily dry bulb temperature $t(c^0)$

	JAN.	FEB.	MAR.	APR.	MAY.	JUN.	JUL.	AUG.	SEP.	OCT.	NOV.	DEC.
1994	9.5	8.3	11.3	17.7	21.4	23.8	24.9	26.2	26.2	22.3	12.2	5.7
1995	8.0	9.4	11.5	14.5	20.8	24.7	25.4	26.2	23.8	18.8	10.4	6.4
1996	6.5	8.7	10.8	13.7	21.6	24.4	26.5	26.3	23.8	18.2	12.7	10.5
Aver.	8	8.8	11.2	15.3	21.66	24.3	25.6	26.23	24.6	19.76	11.76	7.53

Table 2. Monthly average daily relative humidity H_r %

	JAN.	FEB.	MAR.	APR.	MAY.	JUN.	JUL.	AUG.	SEP.	OCT.	NOV.	DEC.
1994	83	79	78	60	55	54	63	61	57	60	82	89
1995	86	78	74	67	59	56	61	61	62	62	73	86
1996	89	81	80	72	58	53	60	62	61	68	73	87
Aver.	86	79.33	77.33	66.33	57.33	54.33	61.33	61.33	60	63.33	76	87.33

Table 3. Monthly average station pressure $P(mb)$

	JAN.	FEB.	MAR.	APR.	MAY.	JUN.	JUL.	AUG.	SEP.	OCT.	NOV.	DEC.
1994	958.9	958.7	957.1	955.7	954.5	951.9	948.8	950.2	954.4	958.2	957.0	962.5
1995	962.3	959.2	957.9	955.1	955.3	952.7	948.8	950.9	954.7	958.3	960.2	963.2
1996	958.3	957.1	954.1	955.8	954.0	952.8	950.3	951.5	954.6	958.2	962.4	960.5
Aver.	959.8	958.3	956.3	955.5	954.6	952.4	949.3	950.8	954.5	958.2	959.8	962.0

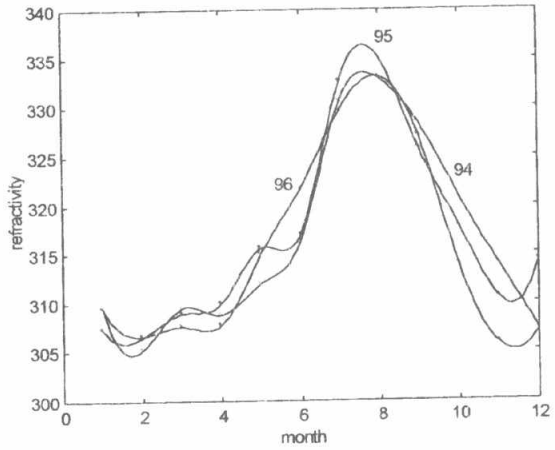

Fig.(1). The monthly variation of refractivity

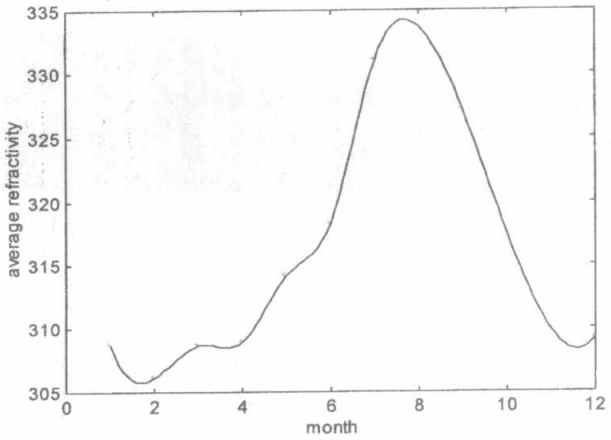

Fig.(2). The average value of refractivity

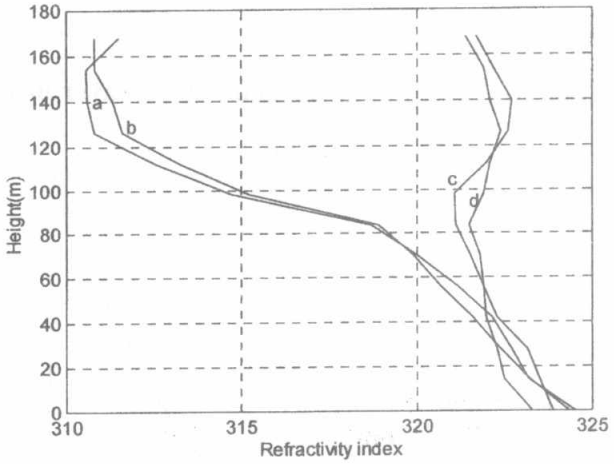

Fig.(3). Refractivity *N* profile.

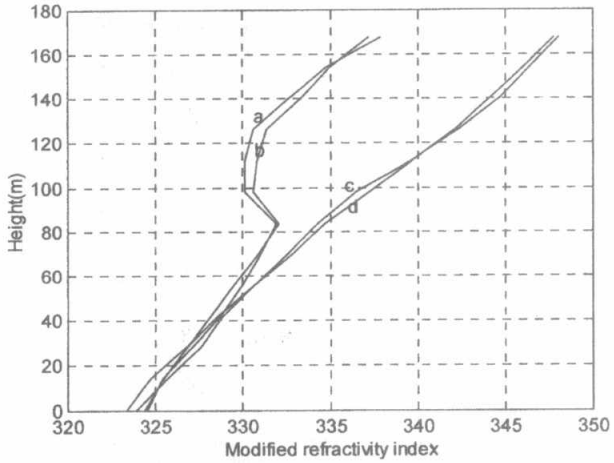

Fig. (4). Modified refractivity *M* profile.

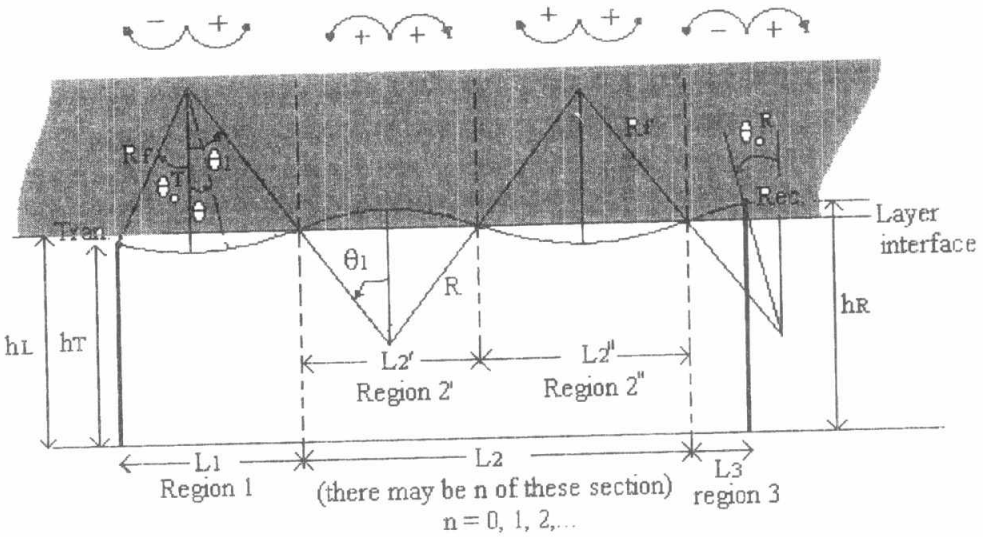

$L_1 = R_f (\sin \theta_1 - \sin \theta_o^T)$

$L_2 = 2 (R + R_f) \sin \theta_1$

$L_3 = R \sin \theta_1 + R \sin \theta_o^R$

$L = L_1 + nL_2 + L_3$

Fig.(5), link geometry with highest terminal above layer interface

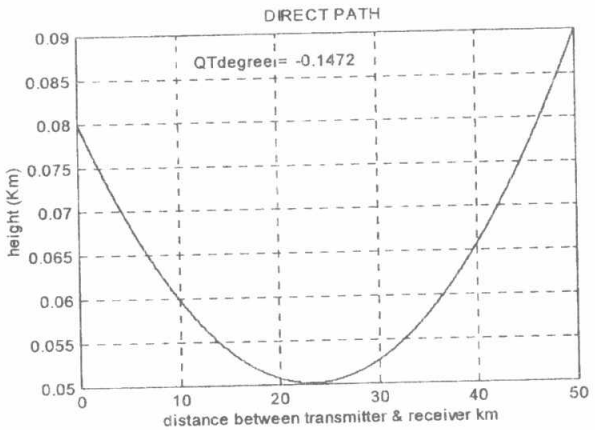

Fig. (6). Direct path for hour 0015.

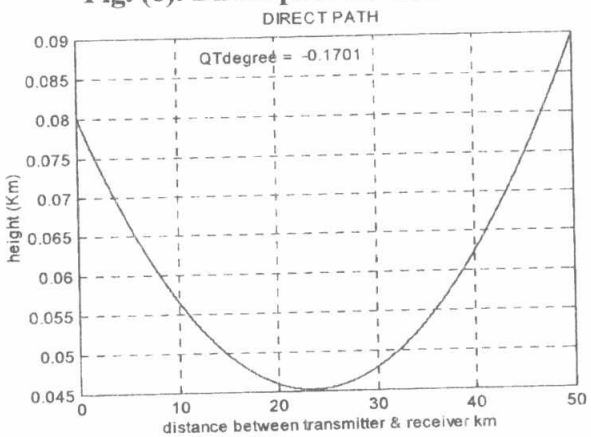

Fig. (7) . Ray path for hour 0035.

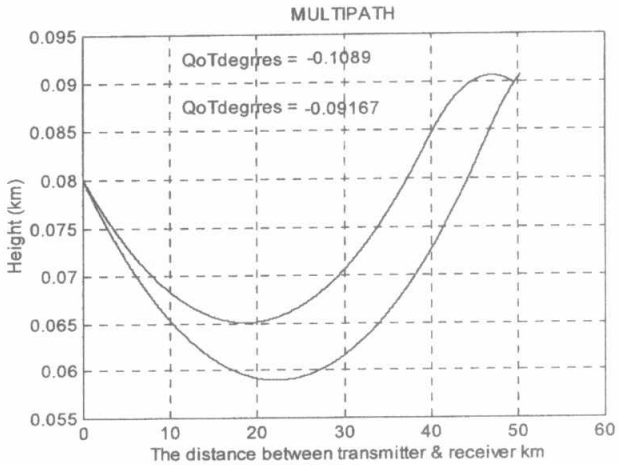

Fig. (8). Multipath rays for the hour 22.30

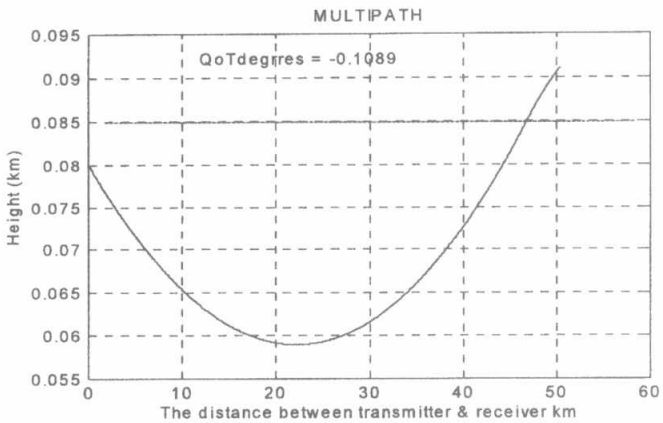

Fig. (9). Ray path for hour 22.55.

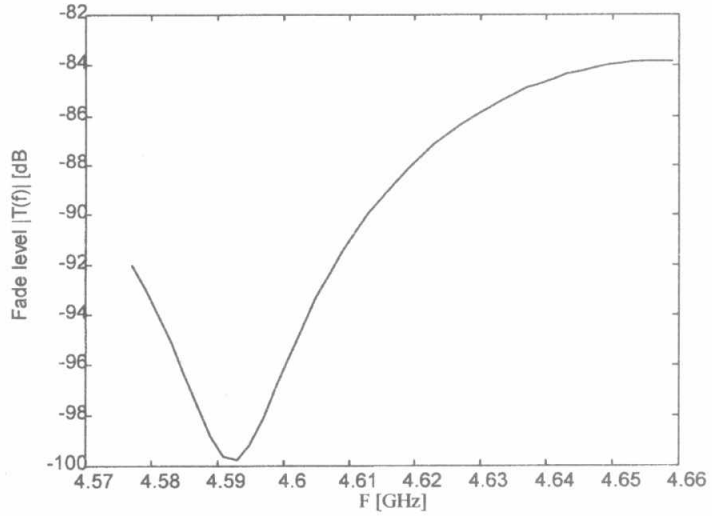

Fig.(10) Frequency selectivity of refractive multipath fading.